Article

Experimental Studies on Model Reference Adaptive Control with Integral Action Employing a Rotary Encoder and Tachometer Sensors

Guo-Qiang Wu [1,2], Shu-Nan Wu [2], Yu-Guang Bai [1,2,]* and Lei Liu [2]

[1] State Key Laboratory of Structural Analysis for Industrial Equipment,
   Faculty of Vehicle Engineering and Mechanics, Dalian University of Technology,
   Dalian 116024, China; E-Mail: gqwu@dlut.edu.cn
[2] School of Aeronautics and Astronautics, Faculty of Vehicle Engineering and Mechanics,
   Dalian University of Technology, Dalian 116024, China;
   E-Mails: wushunan@dlut.edu.cn (S.-N.W.); liulei@dlut.edu.cn (L.L.)

* Author to whom correspondence should be addressed; E-Mail: baiyg@dlut.edu.cn;
   Tel./Fax: +86-411-8470-6213.

Abstract: In this paper, an adaptive law with an integral action is designed and implemented on a DC motor by employing a rotary encoder and tachometer sensors. The stability is proved by using the Lyapunov function. The tracking errors asymptotically converge to zero according to the Barbalat lemma. The tracking performance is specified by a reference model, the convergence rate of Lyapunov function is specified by the matrix Q and the control action and the state weighting are restricted by the matrix Γ. The experimental results demonstrate the effectiveness of the proposed control. The maximum errors of the position and velocity with the integral action are reduced from 0.4 V and 1.5 V to 0.2 V and 0.4 V, respectively. The adaptive control with the integral action gives satisfactory performance, even when it suffers from input disturbance.

1. Introduction

Various electromechanical motors have been used for industrial applications, e.g., electric motors, piezomotors and hydraulic actuators. Generally, it is necessary to enhance the motor performance with the feedback control based on state measurements. Khorrami *et al.*, used linear motors to establish ultra-accurate high-speed six degree-of-freedom manipulation [1]. To measure the angle and speed of motor shafts, rotary encoders and tachometer sensors have been widely used because of their high performance and reliability [2–4].

As digital angle-measuring sensors, rotary encoders consist of optics, mechanics and electronics. Compared to analog angle-measuring sensors, digital rotary encoders have simple structures while preserving high accuracy. In order to achieve accurate motion control, the velocity can be measured by using tachometer sensors which usually consist of tachogenerators and circuits. The tachogenerator can also give the voltage output which is proportional to the speed of the rotational motor.

To achieve precise motion, it is necessary to measure and input both the angle and the speed of motor shafts by employing a rotary encoder and tachometer sensors. Based on the angle and speed sensors, various controllers have been designed for motors [5,6]. Generally, motors can be controlled by conventional PID controllers. Nikulin and Frantsuzova presented a modified PD controller to ensure the desired system speed and damping vibrations [7]. Chaiya and Kaitwanidvilai provided a robust PID controller which could control the motor speed [8], but PID controllers have limited performance in the presence of disturbances and uncertainties. Xu and Yang presented a simple and robust speed control scheme for a permanent magnet synchronous motor to enhance the performance robustness [9]. Nouri *et al.*, proposed a model-following adaptive controller for the speed control of a motor drive system [10]. Melkote and Khorrami proposed adaptive control for direct drive brushless DC motors [11]. Moreover, intelligent algorithms have also been investigated [12–15]. Fallahi and Azadi added neural network sliding mode control to enhance the adaptive control of motors [16]. However, intelligent controllers are usually very complex. It is difficult for engineers to design and optimize intelligent controllers, e.g., Xu and Huang [17] designed an iterative learning controller (ILC), but found that the reference signal had to be pre-filtered in order to satisfy the complex initial conditions of ILC. Furthermore, several accurate models were identified at different voltage ranges, and the iterations were implemented offline.

This paper uses Model Reference Adaptive Control (MRAC), which is a convenient approach to satisfy the requirements of designers [18]. The general idea of MRAC is to create a closed loop regulator with parameters that could be updated to match a desired response. The desired performance is specified by a stable reference model, and the parameters of the adaptive law are adjusted based on the errors between the reference model and the plant, as shown in Figure 1.

Though the adaptive control has shown its effectiveness in achieving robust performance without the knowledge of parameter values, a comprehensive design approach is still necessary for engineering applications. In order to obtain high-performance adaptive control in the presence of disturbances, this paper presents a comprehensive design approach in which both the bandwidth and damping ratio can be included in the proposed controller.

Figure 1. MRAC control sketch of the motor.
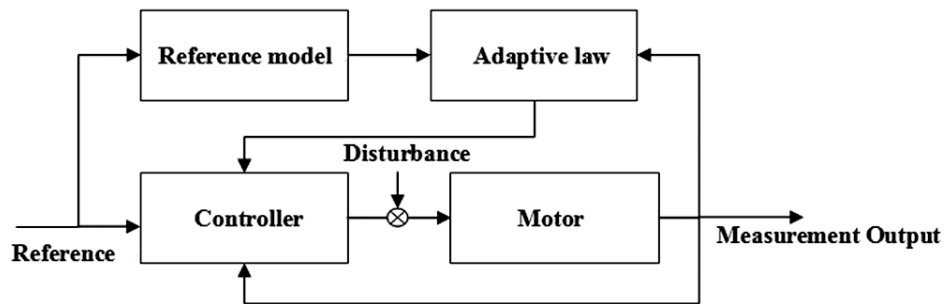
In this paper, two kinds of MRAC are designed and then used on a motor by employing a rotary encoder and tachometer sensors. The tracking error can converge to zero with the integral action in the presence of input disturbances. The experimental results are presented to investigate the effectiveness of the proposed control approach.

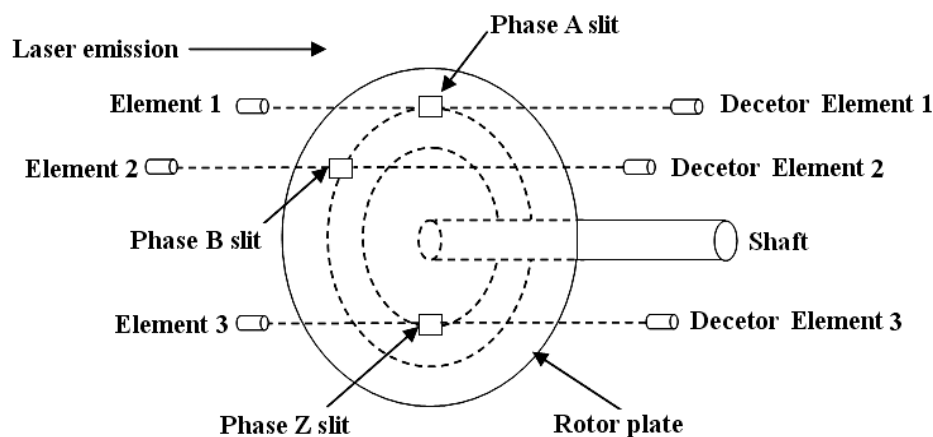## 2. Adaptive Control Design without the Integral Action

2.1. Angle and Speed Sensors

Figure 2 shows the experimental setup. It consists of a DC motor, a computer with LabView software, a drive interface, an amplifier, a tachometer sensor and a rotary encoder. The tachometer sensor is used to measure the rotation speed of the motor shaft. The output voltage of the tachogenertor (*i.e.*, tachometer generator—a device to measure the rotational rate of the motor shaft with the internally generated electrical signal generated by the motor shaft) is proportional to the motor speed. Then, the voltage is applied to the voltmeter in which the dial can be calibrated in speed units (*i.e.*, usually in revolutions per minute (rpm)). In addition, a rotary encoder is used to measure the linear rotation angle of the motor draft. The rotary encoder can convert the ration angle to digital voltage. Thus, both the angle and speed can be measured and controlled.

Figure 2. Sketch of the motor experiment.
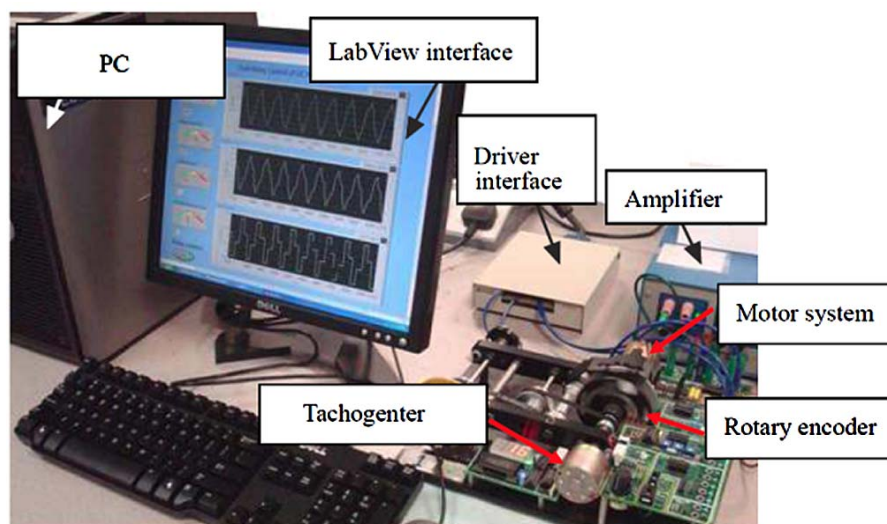
After calibration, the generated voltage is a factor of the motor speed. Then, the motor speed can be fed to the adaptive controller. Next, Figure 3 is given to present the working principle of the rotary encoder in which phase A, phase B, and phase Z are the three-phase models to represent the output signal counts for an incremental encoder [19]. The rotary encoder consists of the main grating, index grating, illuminant and photosensitive device. In this paper, an incremental encoder is used because of its simplification, small size and high-speed response. There is one impulse corresponding to every grating. The summation of impulses represents the angle position of the motor.

Figure 3. Working principle of the rotary encoder.

2.2. Adaptive Controller Design and Stability Proof

This section presents a design method of the adaptive control without the integral action. The stability proof is also presented. To achieve good tracking performance, a MRAC is designed to drive the tracking error to zero. Considering simplification, the transfer function in Equation (1) is used to give the motor dynamics:

$$G_p = \frac{K}{s(1 + \tau s)} \tag{1}$$

where K denotes the DC gain of the velocity transfer function, and τ denotes the time constant. τ are unknown parameters, but their signs can be tested in the experiment. The state space model of Equation (1) can be rewritten in Equation (2):

$$\dot{x} = A_p x + gbu$$
$$y = Cx \tag{2}$$

where:

$$A_p = \begin{bmatrix} 0 & 1 \\ 0 & \dfrac{1}{\tau} \end{bmatrix}, \ b = \begin{bmatrix} 0 \\ 1 \end{bmatrix}, \ g = K, \ C = \begin{bmatrix} 1 & 0 \\ 0 & 1 \end{bmatrix}$$

To specify the desired performance, this paper employs a stable reference model as shown in Equation (3), from which the domain and frequency index can be specified:

$$G_m = \frac{\omega_n^2}{s^2 + 2\xi\omega_n s + \omega_n^2} \tag{3}$$

where ξ is the damping ratio and ω_n is the natural frequency of the reference model. The corresponding state space description can be given as:

$$\begin{pmatrix} \dot{x}_1 \\ \dot{x}_2 \end{pmatrix} = \begin{bmatrix} 0 & 1 \\ -\omega_n^2 & -2\xi\omega_n \end{bmatrix} \begin{pmatrix} x_1 \\ x_2 \end{pmatrix} + \omega_n^2 \begin{bmatrix} 0 \\ 1 \end{bmatrix} r$$

$$y = \begin{bmatrix} 1 & 0 \\ 0 & 1 \end{bmatrix} \begin{pmatrix} x_1 \\ x_2 \end{pmatrix} \tag{4}$$

Equation (4) can be further written as:

$$\dot{x}_m = A_m x_m + g_m b r$$

The following non-adaptive control law is used:

$$u = \theta_x^{*T} x_p + \theta_r^* r \tag{5}$$

where θ_x^* and θ_r^* are the exact gains of the controller Equation (5).

Then, the closed loop system can be given by:

$$\dot{x}_p = \left[A_p + gb\theta_x^{*T} \right] x_p + (g\theta_r^*)br \tag{6}$$

The feedback control system achieves the performance as the matching condition below:

$$A_p + gb\theta_x^{*T} \equiv A_m$$

$$g\theta_r^* \equiv g_m \tag{7}$$

The exact control gains θ_x^{*T} and θ_r^* guarantee that the closed loop system matches the reference model. Actually, the exact values of θ_x^{*T} and θ_r^* are unknown. The controller in Equation (5) can be rewritten to:

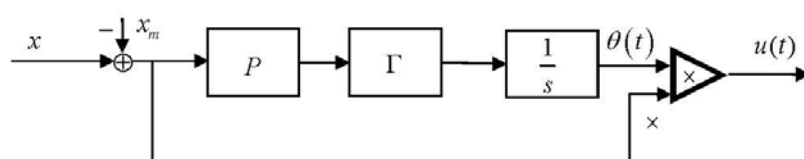$$u = \theta_x^T(x)x_p + \theta_r r(t) \tag{8}$$

where θ_x^T and θ_r can be determined by the adaptation law in Equation (9):

$$\dot{\theta} = \dot{\theta}^* + \dot{\phi} = 2\dot{\phi} = -2\,\mathrm{sgn}(g)\Gamma x e^T P b \tag{9}$$

where θ^* is a constant or the slow time-variant parameter (*i.e.*, $\dot{\theta}^* = \dot{\phi}$).

The adaptive control law is nonlinear, as shown in Figure 4.

Figure 4. Adaptive control block.

To give the tracking performance, the parameter errors ϕ_x and ϕ_r are defined by:

$$\phi_x = \theta_x - \theta_x^*$$
$$\phi_r = \theta_r - \theta_r^*$$

(10)

Then, the closed loop system can be rewritten to:

$$\dot{x}_p = A_p x_p + gb(\theta_x^T(x)x_p + \theta_r r(t))$$
$$= A_m x_p + gb\phi_x^T x_p + gb\theta_r r(t)$$

(11)

Next, let e be the state error and $e = x_p - x_m$.

By comparing the closed loop system in Equation (11) with the reference model in Equation (5), the dynamics of the tracking error e can be given:

$$\dot{e} = A_m e + gb\phi_x^T x_p + gb\theta_r r(t)$$
$$= A_m e + gb\phi^T x$$

(12)

where:

$$\phi = \begin{bmatrix} \phi_r \\ \phi_r \end{bmatrix}, x = \begin{bmatrix} x_p \\ r \end{bmatrix}$$

In the reference model in Equation (4), a stable matrix is used for A_m that can satisfy the algebraic Riccati Equation (13) (*i.e.*, for any symmetric positive definite matrix Q, there is a symmetric positive definite matrix P satisfying Equation (13)):

$$A_m^T P + P A_m = -Q$$

(13)

To prove the stability, a Lyapunov function candidate is used as follows:

$$V(e,\phi) = e^T P e + |g|\phi^T \Gamma^{-1}\phi$$

(14)

where Γ is a positive definite matrix.

The time derivative of the Lyapunov function candidate can be given:

$$\dot{V}(e,\phi) = 2e^T P\dot{e} + 2g\phi^T \Gamma^{-1}\dot{\phi}$$
$$= e^T(A_m^T P + P A_m)e + 2ge^T Pb\phi^T + 2g\phi^T \Gamma^{-1}\dot{\phi}$$
$$= -e^T Qe + 2ge^T Pb\phi^T + 2g\phi^T \Gamma^{-1}\dot{\phi}$$

(15)

Then, Equation (15) can be rewritten to:

$$\dot{V}(e,\phi) = -e^T Qe + 2ge^T Pb\phi^T x - 2\operatorname{sgn}(g)|g|\phi^T x e^T Pb$$
$$= -e^T Qe \le 0$$

(16)

where $g = \operatorname{sgn}(|g|)|g|$, $\phi^T x$ is a scalar.

Thus, the system is stable according to the Lyapunov theorem [20]. Moreover, $\|e\|$, $\dot{e}$, $\|\phi\|$, x_n, θ_x and θ_r are bounded, and:

$$\int_0^\infty e^T Qe\,dt = V_0 - V_\infty < V_0 \le c_1$$

According to the Barbalat lemma [20] here $\dot{V}:[0,+\infty]\to R$ is a uniformly continuous function on $[0,+\infty]$. Supposing $\lim\limits_{t\to\infty}\int_0^t \dot{V}(\tau)d\tau$ exist and be finite. Then, there is $\dot{V}\underset{t\to\infty}{\to}0$.

Here $\dot{e}$ is bounded. Furthermore:

$$\int_0^{\infty} e^T Qe\,dt = V_0 - V_{\infty} < V_0 \le c_1$$

According to the Barbalat lemma, the tracking error e is asymptotically stable and $\lim e = 0$ (*i.e.*, $\lim(\|x_m - x_n\|) = 0$).

To improve the adaptation rate, the proportional action can be added to the adaptive law [14]. Finally, the adaptive law can be given in Equation (17):

$$\overline{\theta} = -(\gamma_1\int\mathrm{sgn}(k_p)\Gamma\overline{\omega}e_1 dt + \gamma_2\,\mathrm{sgn}(k_p)\Gamma\overline{\omega}e_1 \tag{17}$$

where $\gamma_1 = 1$ and $\gamma_2 = 0.5$, and they are used in experiments.

2.3. Experimental Studies of Adaptive Control without the Integral Action

Experimental studies of the adaptive control are now presented. Firstly, ρ can be used to give the convergence rate of the adaptive law, as shown in Equation (18):

$$\rho = \frac{|\dot{V}|}{V} = \frac{\overline{e}^T\overline{Q}\overline{e}}{\overline{e}^T\overline{P}\overline{e} + |g|\overline{\phi}^T\Gamma^{-1}\overline{\phi}} \le \frac{\overline{e}^T\overline{Q}\overline{e}}{\overline{e}^T\overline{P}\overline{e}} \le \frac{\lambda_{\max}(\overline{Q})}{\lambda_{\min}(\overline{P})} = \rho_{\max} \tag{18}$$

After several trials, the reference model is given:

$$A_m = \begin{bmatrix} 0 & 1 \\ -25 & -9 \end{bmatrix},\ \omega = 5,\ \xi = 0.9$$

and the matrix Q is selected as:

$$Q = \begin{bmatrix} 10 & 0 \\ 0 & 1 \end{bmatrix}$$

The selection of Q means that the position tracking is more important than the velocity tracking. Moreover, the sampling interval h should be less than the max interval in order to handle the fastest adaptation rate [18]:

$$h < \frac{1}{20}\frac{1}{\rho_{\max}} = \frac{1}{20}\frac{\lambda_{\min}(\overline{P})}{\lambda_{\max}(\overline{Q})} \tag{19}$$

The matrix P is solved by the ARE in Equation (13):

$$P = \begin{bmatrix} 3.74 & 0.2 \\ 0.2 & 0.078 \end{bmatrix}$$

and denoting Γ:

$$\Gamma = \begin{bmatrix} 1 & 0 & 0 \\ 0 & 0.5 & 0 \\ 0 & 0 & 1 \end{bmatrix}$$

The tracking performance of the adaptive control is shown in Figures 5 and 6. It can be found that the tracking errors of angular position and velocity asymptotically converge to zero in one period, and the maximum tracking errors of position and velocity are 0.4 and 1.5, respectively.

Figure 5. The reference position, the motor position and the tracking error (*i.e.*, (**top**), (**middle**) and (**bottom**), respectively).
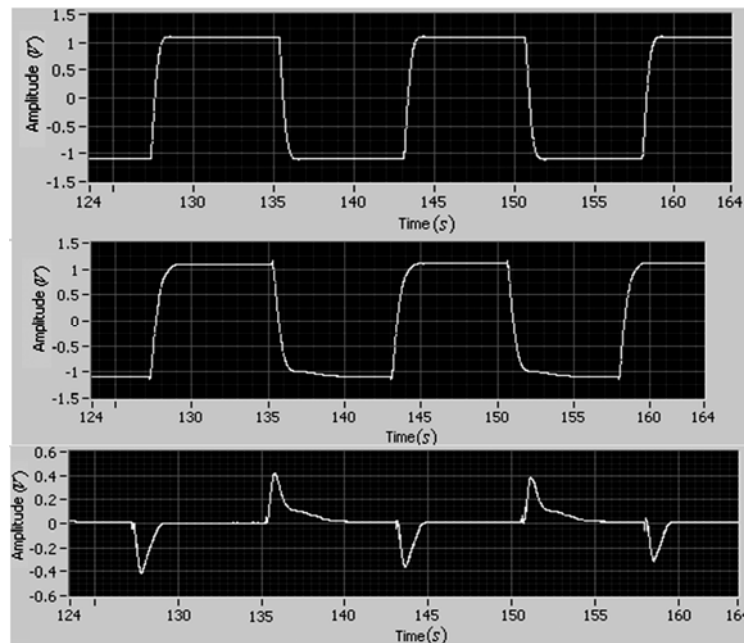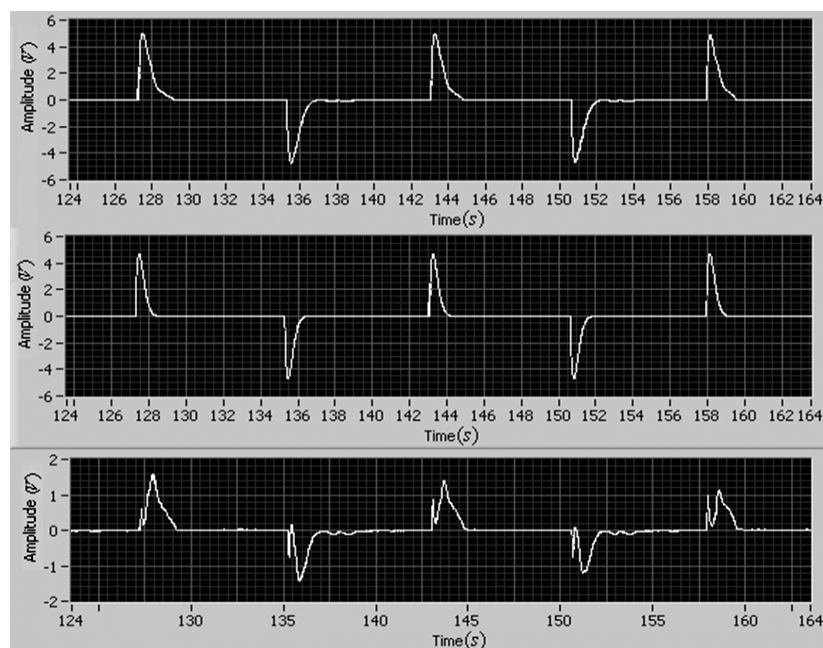

Figure 6. The reference velocity, the motor velocity and the tracking error (*i.e.*, (**top**), (**middle**) and (**bottom**), respectively).

To guarantee the stability of the adaptive control, it is necessary to demonstrate the boundness of $\bar{\theta}$. Figure 7 shows the responses of $\bar{\theta}$. It can be seen that the estimation of $\bar{\theta} = [\theta_{x_1} \ \theta_{x_2} \ \theta_I]$ is bounded.

Figure 7. $\bar{\theta}$ responses under square wave tracking (**top**) and sinusoidal tracking (**bottom**), respectively.
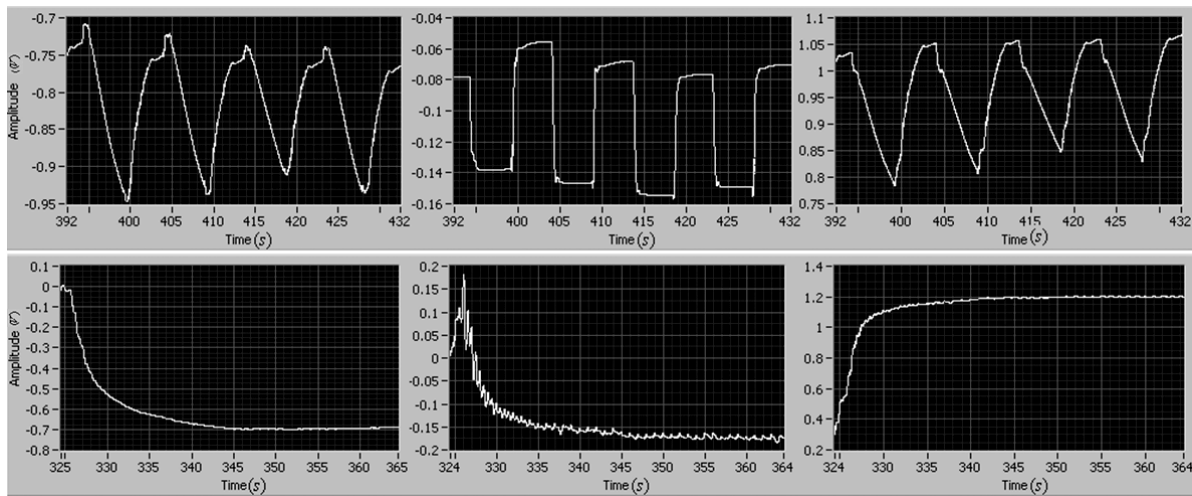
2.4. Investigations of Q and Γ

Q and Γ are two important parameters of the adaptive controller. Different values of Q and Γ are adopted to investigate their influences, here two group values of them are:

$$Q_1 = \begin{bmatrix} 10 & 0 \\ 0 & 1 \end{bmatrix}, P_1 = \begin{bmatrix} 3.74 & 0.2 \\ 0.2 & 0.078 \end{bmatrix}$$

$$Q_1 = \begin{bmatrix} 30 & 0 \\ 0 & 30 \end{bmatrix}, P_1 = \begin{bmatrix} 48.7 & 0.6 \\ 0.7 & 1.778 \end{bmatrix}$$

$$\Gamma_1 = \begin{bmatrix} 1 & 0 & 0 \\ 0 & 0.5 & 0 \\ 0 & 0 & 1 \end{bmatrix}, \Gamma_2 = \begin{bmatrix} 10 & 0 & 0 \\ 0 & 5 & 0 \\ 0 & 0 & 10 \end{bmatrix}$$

where Q_2 is larger than Q_1.

The adaptation rates can be respectively estimated:

$$\rho_1 = \frac{\lambda_{\max}(\bar{Q})}{\lambda_{\min}(\bar{P})} = \frac{10}{0.0669} = 149.5$$

$$\rho_2 = \frac{\lambda_{\max}(\bar{Q})}{\lambda_{\min}(\bar{P})} = \frac{30}{1.77} = 16.9$$

where ρ is the adaptive rate, and ρ_1 is faster than ρ_2.

During experiments, the adaptive control using Q_1 and Q_2 have similar tracking errors, but the control signals are different. Figure 8 shows the voltages of the adaptive control. The control voltage of the adaptive control with (Q_2, Γ_2) is four time larger than that of the adaptive control with (Q_1, Γ_1), though there is no significant differences in the tracking errors.

Figure 8. Control signals under (Q_1, Γ_1) and (Q_2, Γ_2) ((**top**) and (**bottom**), respectively).
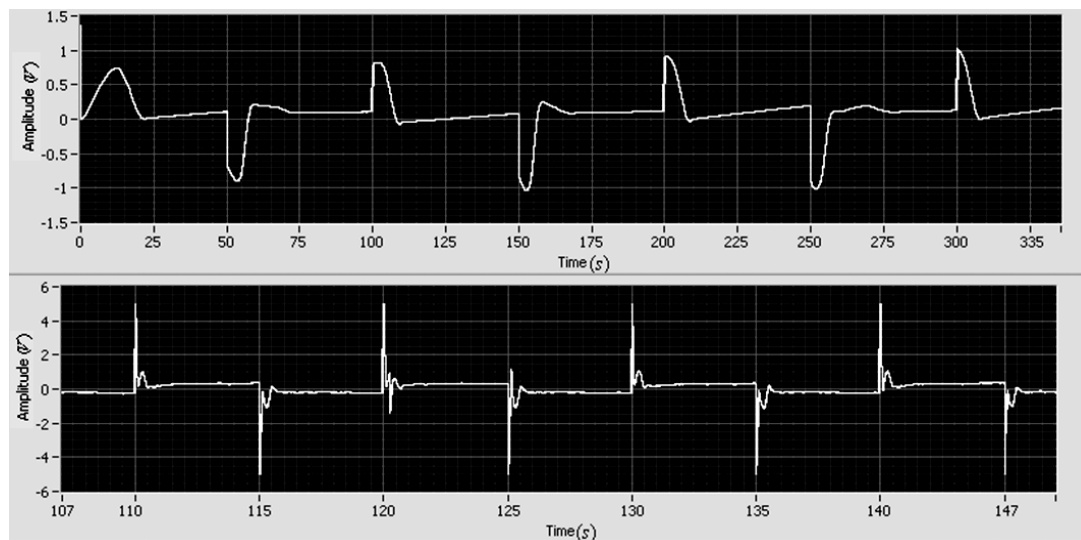
3. Adaptive Control with the Integral Action

3.1. Adaptive Controller Design with the Integral Action and Stability Validation

To further investigate the adaptive control in the presence of disturbances, this section presents the adaptive control with integral action. The integral control action can be added to the adaptive law through Equation (20):

$$\dot{x}_I = x_1 - r \tag{20}$$

where r is the reference signal and x_I is a new state:

$$x_I = \int_0^t x_1 - r d\tau \tag{21}$$

The augmented plant can be rewritten to:

$$\begin{pmatrix} \dot{x}_1 \\ \dot{x}_2 \\ \dot{x}_3 \end{pmatrix} = \begin{bmatrix} 0 & 1 & 0 \\ 0 & \dfrac{1}{\tau} & 0 \\ 1 & 0 & 0 \end{bmatrix} \begin{pmatrix} x_1 \\ x_2 \\ x_3 \end{pmatrix} + g \begin{bmatrix} 0 \\ 1 \\ 0 \end{bmatrix} u + \begin{bmatrix} 0 \\ 0 \\ -1 \end{bmatrix} r \tag{22}$$

Similar to Section 2.2, the control law can be given by:

$$u = \theta_x^{*T} x_p + \theta_I^* x_3 \tag{23}$$

Then the closed loop system can be given as:

$$\begin{pmatrix} \dot{x}_1 \\ \dot{x}_2 \\ \dot{x}_3 \end{pmatrix} = \begin{bmatrix} 0 & 1 & 0 \\ a_{21}^p & a_{22}^p & a_{23}^p \\ 1 & 0 & 0 \end{bmatrix} \begin{pmatrix} x_1 \\ x_2 \\ x_3 \end{pmatrix} + \begin{bmatrix} 0 \\ 0 \\ -1 \end{bmatrix} r \tag{24}$$

where:

$$\begin{bmatrix} 0 & 1 & 0 \\ a_{21}^p & a_{22}^p & a_{23}^p \\ 1 & 0 & 0 \end{bmatrix} = \begin{bmatrix} A_P + gb\theta_x^{*T} & gb\theta_I^* \\ 1 & 0 \end{bmatrix} \tag{25}$$

According to the matching condition in Equation (7), the following equation can be given:

$$\begin{bmatrix} A_P + gb\theta_x^{*T} & gb\theta_I^* \\ 1 & 0 \end{bmatrix} = \overline{A}_m \tag{26}$$

The reference model can be given:

$$\dot{x}_m = \overline{A}_m x_m + \begin{bmatrix} 0 \\ -1 \end{bmatrix} r \tag{27}$$

Actually, the exact value of θ_x^* and θ_I^* cannot be known, so the corresponding estimated values of θ_x and θ_I are used instead. We note that ϕ_x and ϕ_I are the estimate errors as shown in Equation (28):

$$\begin{aligned} \phi_x &= \theta_x(t) - \theta_x^* \\ \phi_I &= \theta_I(t) - \theta_I^* \end{aligned} \tag{28}$$

and

$$\overline{x}_p = \begin{pmatrix} x_1 \\ x_2 \\ x_3 \end{pmatrix}, \ \overline{\varphi} = \begin{bmatrix} \varphi_x \\ \varphi_I \end{bmatrix} \text{ and } \overline{e} = \overline{x}_p - \overline{x}_m$$

where $\theta_x(t)$ and $\theta_I^*(t)$ are the estimated values θ_x^* and θ_I^*, respectively.

Substituting *u* into the plant model in Equation (22), the closed loop can be given:

$$\begin{pmatrix} \dot{x}_p \\ \dot{x}_I \end{pmatrix} = \begin{bmatrix} A_P + gb\theta_x^{*T} & gb\theta_I^* \\ 1 & 0 \end{bmatrix} \begin{pmatrix} x_p \\ x_I \end{pmatrix} + \begin{bmatrix} gb\phi_x & gb\phi_I \\ 0 & 0 \end{bmatrix} \begin{pmatrix} x_p \\ x_I \end{pmatrix} + \begin{bmatrix} 0 \\ -1 \end{bmatrix} r \tag{29}$$

Equation (29) can be rewritten to:

$$\overline{x}_p = \overline{A}_m \overline{x}_p + \begin{bmatrix} gb\phi_x & gb\phi_I \\ 0 & 0 \end{bmatrix} \overline{x}_p + \begin{bmatrix} 0 \\ -1 \end{bmatrix} r \tag{30}$$

The error equation can be given

$$\overline{e} = \overline{A}_m \overline{e} + g\overline{b}\,\overline{\phi}^T \overline{x}_p \tag{31}$$

Choosing the Lyapunov function as Equation (32)

$$V = \overline{e}^T \overline{P}\overline{e} + |g|\overline{\varphi}^T \Gamma^{-1} \overline{\varphi} \tag{32}$$

Then, the time derivative of *V* can be obtained:

$$\frac{dV}{dt} = 2\overline{e}^T \overline{P}\overline{e} + 2|g|\overline{\varphi}^T \Gamma^{-1}\overline{\varphi} = \overline{e}^T (\overline{A}_m^T \overline{P} + \overline{P}\overline{A}_m)\overline{e} + 2g\overline{e}^T \overline{P}\overline{b}\,\overline{\phi}^T \overline{x}_p + 2|g|\overline{\varphi}^T \Gamma^{-1}\overline{\varphi} \tag{33}$$

Denote that the adaptive law is:

$$\overline{\phi} = \begin{bmatrix} \dot{\theta}_x(t) \\ \dot{\theta}_I(t) \end{bmatrix} = -\text{sgn}(g)\Gamma \begin{bmatrix} x_p \\ x_I \end{bmatrix} \overline{e}^T \overline{P} \overline{b} \tag{34}$$

Then, $\overline{P}$ can be gotten from the ARE Equation (35):

$$\overline{A}_m^T \overline{P} + \overline{P} \overline{A}_m = -\overline{Q} \tag{35}$$

where $\overline{Q}$ is a positive definite symmetric matrix, so the following Equation (36) can be obtained:

$$\frac{dV}{dt} = -\overline{e}^T \overline{Q} \overline{e} \le 0 \tag{36}$$

It can be concluded that the closed loop is Lyapunov stable, and $\overline{e}$ and $\overline{\varphi}$ are bounded. As in Section 2.2, the tracking error $\overline{e}$ is asymptotically stable.

The adaptive control law is shown as follows:

$$u = \theta_x^T x_p + \theta_I x_I \tag{37}$$

$$\dot{\theta} = \begin{bmatrix} \dot{\theta}_x \\ \dot{\theta}_I \end{bmatrix} = -\text{sgn}(g)\Gamma \begin{bmatrix} x_p \\ x_I \end{bmatrix} \overline{P} \overline{b} \tag{38}$$

where $\overline{\phi} \approx \dot{\theta}$, P can be computed through the ARE.

3.2. Reference Model Design

This section presents how to specify the requirements through the reference model G_m. Firstly, the third order model in Equation (39) is given to satisfy the matching condition of the adaptive integral control. To specify performance indexes such as the bandwidth and damping ratio, the reference model G_m can be approximated by the second order model G_{m1}:

$$G_m = G_{m1} \cdot G_{m2} = \frac{w_n^2}{s^2 + 2\zeta w_n + w_n^2} \cdot \frac{a_m}{s + a_m} = \frac{a_m w_n^2}{(s + P_1)(s + \overline{P_1})(s + a_m)} \tag{39}$$

where $\|a_m\| \ge 3\|p_1\|$ (*i.e.*, p_1 and $\overline{p_1}$ are dominant poles which mainly contribute to the dynamic response of the reference model.)

To satisfy the matching conditions, the reference model is:

$$\begin{pmatrix} \dot{x}_1 \\ \dot{x}_2 \\ \dot{x}_3 \end{pmatrix} = \begin{bmatrix} 0 & 1 & 0 \\ a_{21} & a_{22} & a_{23} \\ 1 & 0 & 0 \end{bmatrix} \begin{pmatrix} x_1 \\ x_2 \\ x_3 \end{pmatrix} + \begin{bmatrix} 0 \\ 0 \\ -1 \end{bmatrix} r$$

$$y = [1 \quad 0 \quad 0] \begin{pmatrix} x_1 \\ x_2 \\ x_3 \end{pmatrix} \tag{40}$$

Both Equations (39) and (40) describe the same reference model. The state space Equation (40) is transformed into the transfer function:

$$G_m = D + C(sI - A)^{-1} B = \begin{bmatrix} 1 & 0 & 0 \end{bmatrix} \left(sI_{3\times3} - \begin{bmatrix} 0 & 1 & 0 \\ a_{21} & a_{22} & a_{23} \\ 1 & 0 & 0 \end{bmatrix} \right)^{-1} \begin{bmatrix} 0 \\ 0 \\ -1 \end{bmatrix} = \frac{-a_{23}}{s^3 - a_{22}s^2 - a_{21}s - a_{23}} \qquad (41)$$

Compared with the transfer function in Equation (39), it is seen that:

$$\begin{aligned} a_{21} &= -(\omega_n^2 + 2\zeta\omega_n a_m) \\ a_{22} &= -(2\zeta\omega_n + a_m) \\ a_{23} &= -\omega_n^2 a_m \end{aligned} \qquad (42)$$

The dynamics of the reference model should match the dynamics (*i.e.*, natural frequency) of the motor system and the sampling capability. After testing several groups of values, $\zeta = 0.9$, $w_n = 3$ and $a_m = 9$ are chosen in this paper. Then, there are $a_{21} = -57.6$, $a_{22} = -14.4$ and $a_{23} = -81$. The reference model can be rewritten to:

$$\begin{pmatrix} \dot{x}_1 \\ \dot{x}_2 \\ \dot{x}_3 \end{pmatrix} = \begin{bmatrix} 0 & 1 & 0 \\ -57.6 & -14.4 & -81 \\ 1 & 0 & 0 \end{bmatrix} \begin{pmatrix} x_1 \\ x_2 \\ x_3 \end{pmatrix} + \begin{bmatrix} 0 \\ 0 \\ -1 \end{bmatrix} r$$

$$y = \begin{bmatrix} 1 & 0 & 0 \end{bmatrix} \begin{pmatrix} x_1 \\ x_2 \\ x_3 \end{pmatrix} \qquad (43)$$

The step responses of G_{m1} and G_m are shown in Figure 9. It is seen that G_{m1} contributes most of the response for the third order reference model G_m. The fast dynamics of the reference model is influenced by the part $a_m/(s + a_m)$:

Figure 9. Step responses of G_m (solid line) and G_{m1} (star line).
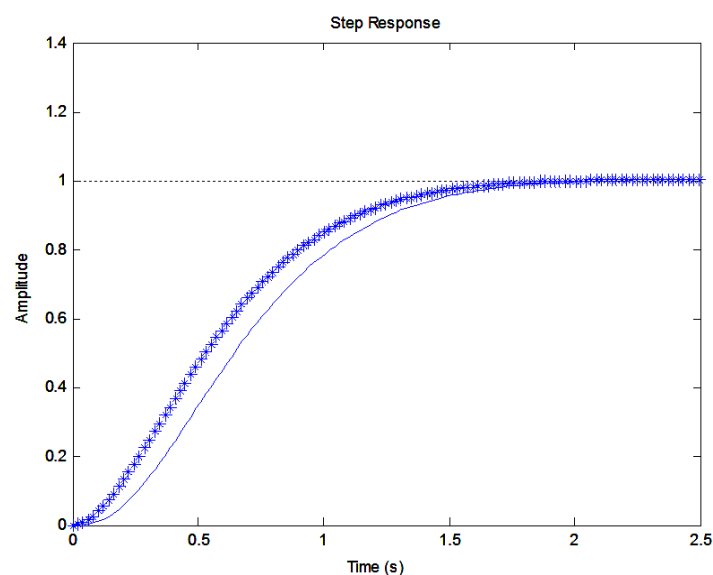
3.3. Experimental Studies on the Adaptive Control with Integral Action

In Section 2, it has been found that a large $\overline{Q}$ results in fast convergence while needing strong action and fast sampling rate. In contrast, a small $\overline{Q}$ results in slow convergence and cannot give better performance. A suitable $\overline{Q}$ should be given to satisfy the convergence rate and hardware limitation.

After trials, $\overline{Q}$ is adopted:

$$\overline{Q} = \begin{bmatrix} 15 & 0 & 0 \\ 0 & 10 & 0 \\ 0 & 0 & 15 \end{bmatrix}$$

Then, $\overline{P}$ can be computed:

$$\overline{P} = \begin{bmatrix} 32.9913 & 0.7111 & 34.4582 \\ 0.7111 & 0.3966 & 0.0926 \\ 33.4582 & 0.0926 & 62.9307 \end{bmatrix}$$

In addition, Γ is adopted:

$$\Gamma = \begin{bmatrix} 4 & 0 & 0 \\ 0 & 2.5 & 0 \\ 0 & 0 & 4 \end{bmatrix}$$

The experimental results of the position and velocity tracking are shown in Figures 10 and 11, respectively. The maximum tracking errors of position and rate are less than 0.2 V and 0.4 V, respectively.

Figure 10. The reference position, the motor position and the tracking error (*i.e.*, **(top)**, **(middle)** and **(bottom)**, respectively).
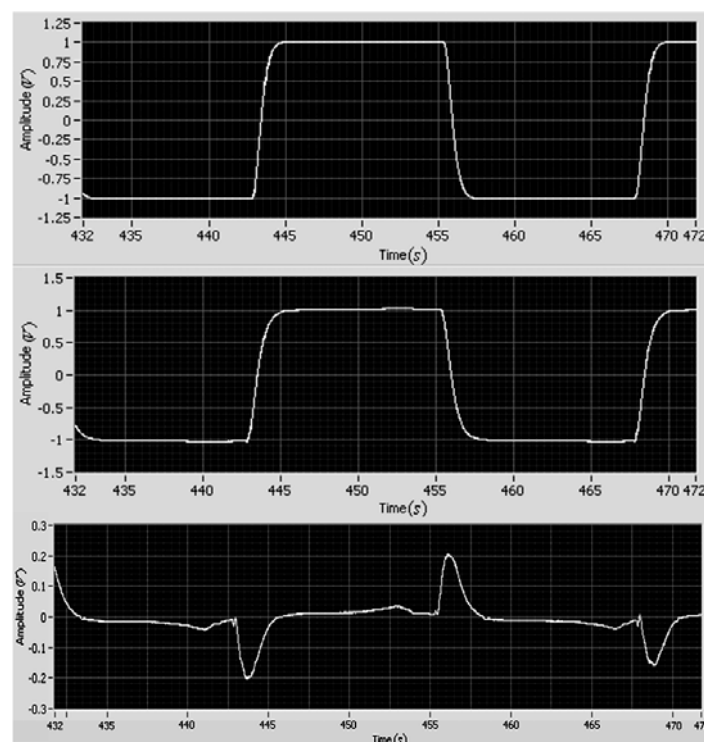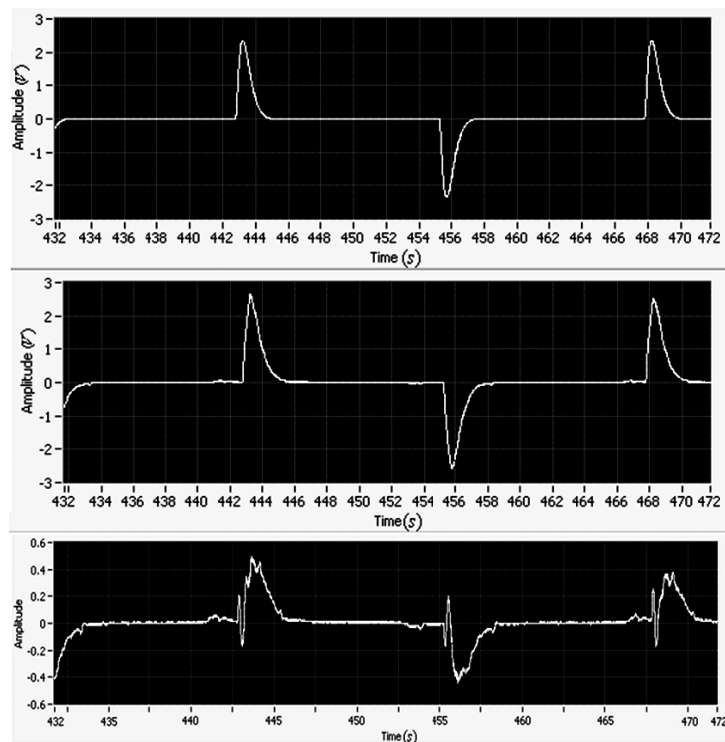
Figure 11. The reference velocity, the motor velocity and the tracking error (*i.e.,* (**top**), (**middle**) and (**bottom**), respectively).

As shown in Figure 12, the magnitude of the controller is less than 0.85 V, and there is no chatter phenomenon. Compared to the former adaptive control without the integral action, the case with the integral adaptive control can reduce the reference errors of position and velocity by as much as 50%. The experimental results demonstrate that the integral action is effective to improve the tracking performance.

Figure 12. Control signal.
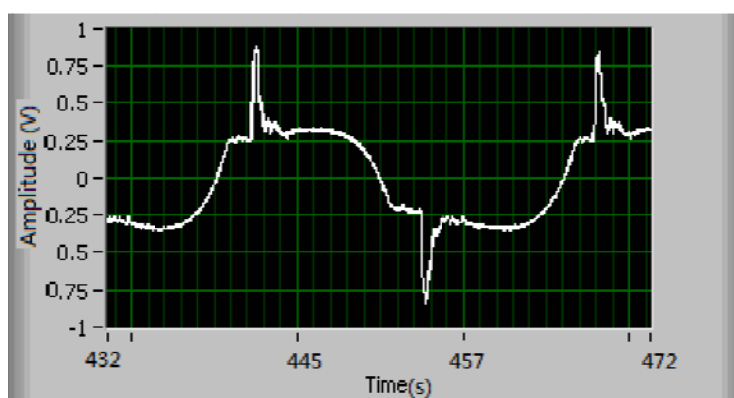
3.4. Tracking Performance with Input Disturbance

In order to investigate the performance of the adaptive control, the input disturbance is considered in this section. The square wave disturbance with magnitude 1 is adopted. The reference is also square wave. During the experiment, the disturbance is added by using a LabView block as an input disturbance. The disturbance enters the close loop systems as the reference signal enters. The tracking errors of position and velocity are shown in Figure 13. It is seen that the maximum position and

velocity tracking errors are less than 0.2 and 1, respectively. Also, it can be found that there is no difference between the two results of the position tracking errors shown in Figures 10 and 13, respectively. The position error is the most important one for the motor tracking in this paper, thus it can be concluded that the degradation of tracking performance is not significant. The experimental result indicates that the adaptive control with the integral action suppresses disturbance and tracks the reference simultaneously.

Figure 13. Tracking errors of position (**top**) and velocity (**bottom**).
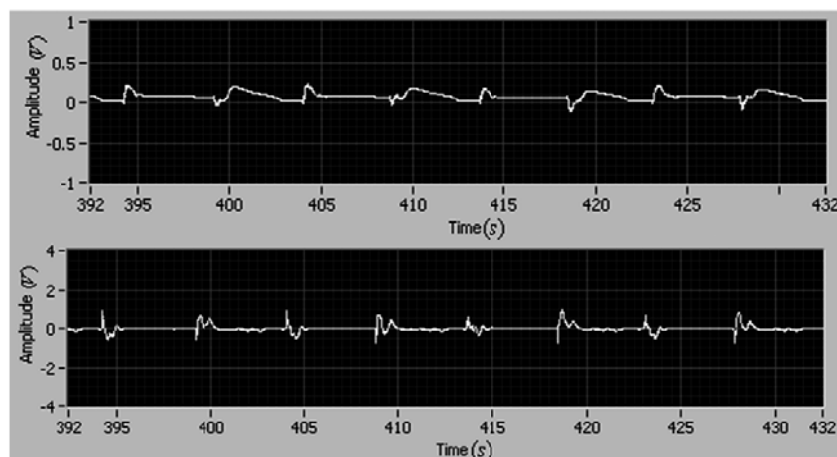
3.5. Comparison between Experiment and Simulation Results

Finally, a comparison between experiment and simulation results is presented in this paper. According to the motor manual, the time constant is 0.25. The DC gain is 5.2. Figure 14 shows the comparison between experiment and simulation results.

Figure 14. Comparison of experiment and simulation results (case I: experimental results of Adaptive control; case II: experimental results of adaptive control with integral action; and case III: Simulation results of simulation of adaptive control with integral action).
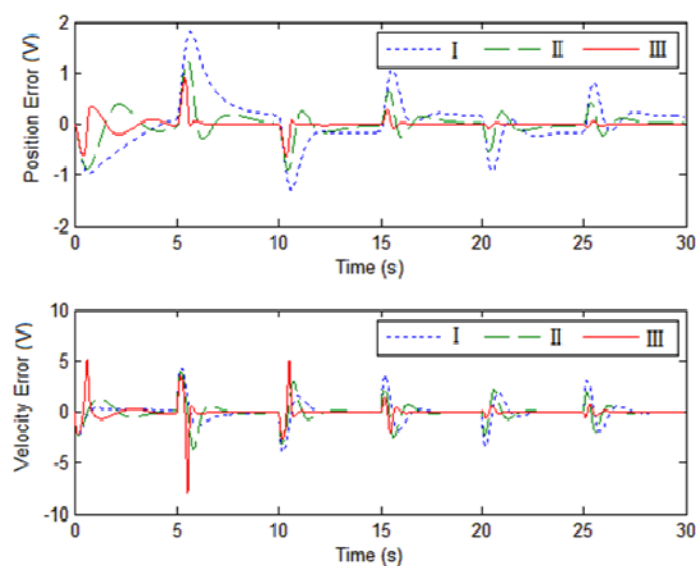
The simulation and experiment have similar responses. The tracking errors of the position and velocity from experiment study are larger than that from simulation study. In the three cases, all the tracking errors asymptotically converge (*i.e.*, the stability can hold). The simulation of the proposed adaptive control with the integral action gives the best performance. The tracking error from simulation study can converge to zero, but the tracking errors from experiment study cannot converge to zero due to the friction, the sensor noise and the motor dead-zone. In the experiment study, the performance degradation is acceptable.

4. Conclusions

In order to accurately control motors, this paper employs both a rotary encoder and tachometer sensors to measure the angle-position and speed, respectively. Based on the measurements, two adaptive controllers are developed for the motor system. The stability and convergence are validated by the Lyapnov theorem and Barbalat lemma. Then, the control system is implemented by using Labview. Experimental results indicate that the tracking errors of the motor position and velocity asymptotically converge to their error ranges. In the presence of disturbances, the adaptive controller with integral action presents better performance than the case without integral action.

State estimation approaches are encouraged to investigate for possible output feedback control. In this paper, the proposed adaptive controllers needs full state information, but actually some states (e.g., motor velocity) are not provided. Thus, the state estimation must be designed in the possible output feedback control.

References

1. Khorrami, F.; Ksishnamurthy, P.; Melkote, H. *Modeling and Adaptive Nonlinear Control of Electric Motors*; Springer: Berlin, Germany, 2003.
2. Casey, N.F.; Laura, P.A.A. A review of the acoustic emission monitoring of wire rope. *Ocean Eng.* **1997**, *24*, 935–947.
3. Casey, N.F.; Taylor, J.L.; Holford, K.M. Wire break detection during tensile fatigue testing of 40 mm wire rope. *Br. J. Non-Destr. Test.* **1985**, *30*, 338–341.
4. Casey, N.F.; White, H.; Taylor, J.L. Frequency analysis of the signals generated by the failure of constituent wires of a wire rope. *NDT Int.* **1985**, *56*, 339–344.
5. Hu, D.J.; Burg, T. *Nonlinear Control of Electric Machinery*; Maecel Dekker Inc.: New York, NY, USA, 1998.
6. Wiberg, J. Controlling a Brushless DC Motor in a Shift by Wire System. MS.c. Thesis, Linkoping University, Linkoping, Sweden, December 2003.

7. Nikulin, G.L.; Frantsuzova, G.A. Synthesis of an electric-power steering control system, optoelectronics. *Instrum. Data Process.* **2008**, *44*, 454–458.

8. Chaiya, U.; Kaitwanidvilai, S. Fixed-Structure Robust DC Motor Speed Control. In Proceeding of the International Multiconference of Engineers and Computer Scientists, Hong Kong, China, 18–20 March 2009.

9. Xu, D.G.; Yang, G. A simple and robust speed control scheme of permanent magnet synchronous motor. *J. Control. Theory A* **2004**, *2*, 165–168.

10. Nouri, K.; Dhaouadi, R.; Braiek, N. Adaptive control of a nonlinear DC motor drive using recurrent neural networks. *Appl. Soft Comput.* **2008**, *8*, 371–382.

11. Melkote, H.; Khorrami, F. Nonlinear adaptive control of direct drive brushless DC motors and applications to robotic manipulators. *IEEE Trans. Mechatron.* **1999**, *4*, 71–81.

12. Chen, C.W. A fuzzy AHP-based fault diagnosis for semiconductor lithography process. *Int. J. Innov. Comput. I* **2011**, *7*, 805–816.

13. Chen, C.W. Stability analysis and robustness design of nonlinear systems: An NN-based approach. *Appl. Soft. Comput.* **2011**, *11*, 2735–2742.

14. Chen, C.W. Stabilization of adaptive neural network controllers for nonlinear structural systems using a singular perturbation approach. *J. Vib. Control* **2011**, *17*, 1241–1252.

15. Chen, C.W. GA-based adaptive neural network controllers for nonlinear systems. *Int. J. Innov. Comput. I* **2010**, *6*, 1793–1803.

16. Fallahi, M.; Azadi, S. Adaptive Control of a DC Motor Using Neural Network Sliding Mode Control. In Proceedings of the International Multiconference of Engineers and Computer Scientists, Hong Kong, China, 18–20 March 2009.

17. Xu, J.-X.; Huang, D.; Venkataramanan, V.; Tuong, H.T.C. Extreme Precise Motion Tracking of Piezoelectric Positioning Stage Using Sampled-Data Iterative Learning Control. In Proceeding of 37th Annual Conference on IEEE Industrial Electronics Society (IECON 2011), Melbourne, Australia, 7 November 2011; pp. 3376–3381.

18. Astrom, K.J.; Wittenmark, B. *Adaptive Control*, 2nd ed.; Addison Wesley: New York, NY, USA, 1994.

19. Dursun, M.; Ozden, S. Design of Monitoring System for Linear Switched Reluctance Motor with Quadrature Encoder and Current Sensors. In Proceedings of the 4th IEEE International Conference on Computer Science and Information Technology (ICCSIT 2011), Chengdu, China, 10 June 2011; pp. 543–546.

20. Khail, H.K. *Nonlinear Systems*, 3rd ed.; Prentice Hall: London, UK, 2002.